Inhibition of human tumor growth in mice by an oncolytic herpes simplex virus designed to target solely HER-2-positive cells

Laura Menotti[a], Giordano Nicoletti[b], Valentina Gatta[a], Stefania Croci[c], Lorena Landuzzi[b], Carla De Giovanni[c], Patrizia Nanni[c], Pier-Luigi Lollini[d], and Gabriella Campadelli-Fiume[a,1]

[a]Department of Experimental Pathology, Section on Microbiology and Virology, University of Bologna, Via San Giacomo 12, 40126 Bologna, Italy; [b]Laboratory of Oncologic Research, Rizzoli Orthopaedic Institute, Viale Filopanti 22, 40126 Bologna, Italy; and [c]Department of Experimental Pathology, Section of Cancer Research, and [d]Department of Hematology and Oncological Sciences, University of Bologna, Viale Filopanti 22, 40126 Bologna, Italy

Edited by Thomas E. Shenk, Princeton University, Princeton, NJ, and approved March 25, 2009 (received for review December 3, 2008)

Oncolytic virotherapy exploits the ability of viruses to infect, replicate into, and kill tumor cells. Among the viruses that entered clinical trials are HSVs. HSVs can be engineered to become tumor-specific by deletion of selected genes or retargeting to tumor-specific receptors. A clinically relevant surface molecule is HER-2, hyperexpressed in one fourth of mammary and ovary carcinomas, and associated with high metastatic ability. As a previously undescribed strategy to generate HSV recombinants retargeted to HER-2 and detargeted from natural receptors, we replaced the Ig-folded core in the receptor-binding virion glycoprotein gD with anti-HER-2 single-chain antibody. The recombinant entered cells solely via HER-2 and lysed HER-2–positive cancer cells. Because of the high specificity, its safety profile in i.p. injected mice was very high, with a $LD_{50} > 5 \times 10^8$ pfu, a figure at least 10,000-fold higher than that of corresponding WT-gD carrying virus ($LD_{50} \approx 5 \times 10^4$ pfu). When administered intratumorally to nude mice bearing HER-2–hyperexpressing human tumors, it strongly inhibited progressive tumor growth. The results provide a generally applicable strategy to engineer HSV recombinants retargeted to a wide range of receptors for which a single-chain antibody is available, and show the potential for retargeted HSV to exert target-specific inhibition of human tumor growth. Therapy with HER-2-retargeted oncolytic HSV could be effective in combined or sequential protocols with monoclonal antibodies and small inhibitors, particularly in patients resistant to HER-2-targeted therapy because of alterations in HER-2 signaling pathway, or against brain metastases inaccessible to anti-HER-2 antibodies.

mammary carcinoma | ovary carcinoma | retarget | tropism

Since the pioneering observation that a genetically modified herpes simplex virus (HSV) exerts a therapeutic effect against glioblastoma (1), oncolytic virotherapy has entered clinical experimentation (2–7). Ideally, the oncolytic virus is genetically reprogrammed to target tumor cells and spare normal cells (4, 8, 9). Because viruses use cell surface molecules as portal of entry into the cell, an effective strategy to generate tumor-specific viruses is to retarget them to receptors unique, or overexpressed in the tumor cell, and detarget them from natural receptors (4, 10–13). A clinically relevant candidate is the HER-2 tyrosine kinase expressed in human breast and ovary carcinomas, which altogether account for >200,000 new cancer cases each year in the U.S. (14). HER-2 hyperexpression is found in approximately one fourth of all cases, and correlates with an aggressive tumor behavior (15). Breast cancers hyperexpressing HER-2 are currently treated with HER-2 targeted monoclonal antibodies, like trastuzumab, or with small molecule tyrosine kinase inhibitors, like lapatinib (16, 17). However, only a subset responds to current targeted therapy, mainly because of alterations in HER-2 signaling pathway; thus, illustrating the pressing need for novel therapeutic approaches against this tumor target (18). Despite its clinical relevance, few efforts were made so far to generate HER-2 specific oncolytic viruses (19, 20).

Among oncolytic viruses, HSVs emerged as a promising platform, and entered clinical trials against malignant gliomas (2, 3). The mutants deleted of the viral $\gamma_1$34.5 gene discriminate between normal and tumor cells, because their replication is suppressed by activated protein kinase R present in normal cells. In ≈25% of malignant gliomas, this pathway is suppressed, allowing the virus to replicate in the tumor. The second approach to engineer tumor-specific HSVs consisted in retargeting to novel receptors (10). WT-HSV-1 enters cells via the interaction of the virion envelope glycoprotein gD with either nectin1 or herpesvirus entry mediator (HVEM) (21–24). HSV-1 recombinants were successfully retargeted to IL-13 receptor α2, abundant in gliomas, by insertion of IL-13 at gD N terminus (10). Our laboratory constructed HER-2-retargeted HSVs by inserting in gD a single-chain antibody (scFv) to HER-2 (25, 26); this accomplishment was a surprising result, because the insert was almost as large as gD ectodomain itself.

Although the HVEM tropism was readily abolished by deletion of the most N-terminal region (12, 26), a major difficulty in generating fully retargeted HSVs has been the abolition of nectin1 tropism. In IL-13-retargeted HSV, detargeting from nectin1 was achieved by a point mutation (12). In the HER-2-retargeted R-LM113, the N-terminal deletion extended to residue 38, and overall access to the nectin1-binding site was simply hindered by the large insert (26). Therefore, R-LM113 was potentially at risk of reversion to nectin1 usage. Here, we constructed a HER-2-retargeted HSV (R-LM249), in which the gD Ig-core (amino acids 61–218), that carries residues critical to nectin1 interaction (24), was replaced with the Ig-folded scFv to HER-2. The design was prompted by Zhou and Roizman discovery (27) that a naturally arisen virus contained a peculiar form of gD split into 2 fragments with a spontaneous deletion of Ig-core. Because this region is likely to serve as a scaffold, we replaced it with scFv to HER-2. The replacement was remarkable, because it involved half of gD ectodomain. In contrast to split gD (27), R-LM249 gD carried all domains in a single peptide. By this approach, we achieved 4 objectives: (*i*) provided trastuzumab scFv as a novel ligand and, thus, retargeted HSV to HER-2; (*ii*) provided an Ig-folded scaffold; (*iii*) simultaneously

Author contributions: L.M., C.D.G., P.N., P.-L.L., and G.C.-F. designed research; L.M., G.N., V.G., S.C., L.L., C.D.G., and P.N. performed research; L.M., C.D.G., P.N., P.-L.L., and G.C.-F. analyzed data; and L.M., C.D.G., P.N., P.-L.L., and G.C.-F. wrote the paper.

The authors declare no conflict of interest.

This article is a PNAS Direct Submission.

Freely available online through the PNAS open access option.

[1]To whom correspondence should be addressed. E-mail: gabriella.campadelli@unibo.it.

This article contains supporting information online at www.pnas.org/cgi/content/full/0812268106/DCSupplemental.

MICROBIOLOGY

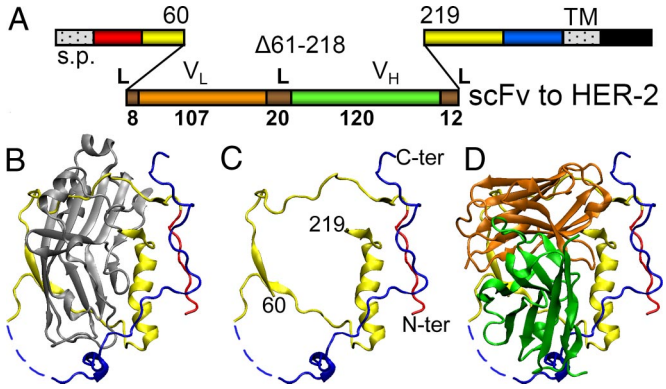

Fig. 1. Linear map and 3D structure of chimeric R-LM249 gD. (*A*) Linear map of R-LM249 gD. The size of the scFv insert is drawn to scale. (L) linkers; s.p., signal peptide; TM, transmembrane domain; V_L and V_H, variable light and heavy chains; Δ, deletion. Numbers in boldface indicate the length in amino acid residues. Plain numbers refer to amino acid residues according toWT gD coordinates. Color code as in *B–D*. (*B*) Monomeric crystal structure of gD ectodomain, solved from an artificial dimer (PDB entry 2C36) (42): red, N terminus (amino acids 23–32); blue, C terminus (257–307); dashed blue line, nonresolved residues; gray, amino acids 61–218, encompassing the Ig core; yellow, other portions. (*C*) As in *B*, without amino acid 61–218. (*D*) Diagram showing the V_L (orange) and V_H (green) structure of trastuzumab scFv to HER-2 (PDB entry 1N8Z) drawn to scale and superimposed to gD as in *C*. The relative orientation of the 2 structures is arbitrary. Molecular graphics were produced with visual molecular dynamics (VMD) (43).

detargeted from nectin1 and HVEM; and (*iv*) prevented any possible reversion to WT tropism. We report on R-LM249 safety profile and in vivo efficacy in inhibiting growth of HER-2-expressing human tumor cells.

Results

Construction of a Redirected HSV Recombinant by Replacement of a gD Portion with scFv to HER-2. As a strategy to construct a HSV recombinant simultaneously retargeted to the selected HER-2 surface molecule and detargeted from the natural receptors nectin1 and HVEM, we engineered a single peptide gD, in which the natural Ig-folded core (half of gD ectodomain, amino acid 61–218) was replaced with the Ig-folded scFv directed to HER-2. The gene encoding the chimeric gD was recombined in the HSV genome, in place of the natural gD gene. The linear map of R-LM249 gD is shown in Fig. 1. For recombination, we made use of HSV-BAC technology in *Escherichia coli* (Fig. S1), through a multiple step engineering. Briefly, we first replaced the gD ORF with a Kanamycin resistance gene flanked by FLP recombinase target (FRT) sites, by ET-cloning. We then removed the antibiotic resistance cassette by FRT targeted recombination, and engineered the EGFP gene under the immediate early α27 promoter within the BAC sequences (26). This insertion site allows removal of EGFP and BAC sequences by Cre-mediated recombination, once it is no longer required. Last, we recombined the recipient HSV-BAC genome with a shuttle vector containing the chimeric gD plus upstream and downstream flanking sequences. R-LM5 was constructed by a similar strategy (26); it contains the EGFP gene within the BAC sequences, and differs from R-LM249 for carrying WT-gD instead of chimeric gD. Fig. 1 *B–D* shows the crystal structure of gD (*B*), the gD portions that were maintained in gD-R-LM249 (*C*), and a diagram in which the gD remaining portions were overlaid with the scFv from trastuzumab (*D*).

R-LM249 Is Retargeted to HER-2 and Detargeted from Nectin1 and HVEM. To assess R-LM249 tropism, we first made use of cell transfectants expressing a single receptor. The parental J cells express no HSV receptor, and are not infected by WT-HSV. J-HER-2, J-HVEM, J-hNectin1, and J-mNectin1 cells express human HER-2, human HVEM/HveA (herpesvirus entry mediator), human or mouse Nectin1, respectively (21, 22). Infection was detected as EGFP fluorescence. The results show that the only cells infected by R-LM249 were those expressing HER-2 (Fig. 2*A*). J-nectin1 and J-HVEM cells were completely resistant to infection by R-LM249, in contrast with WT-HSV that readily infected both cells (21, 25). Next, we infected cell lines of different species, all susceptible to WT-HSV, namely the human HEp-2 and I-143-tk$^-$ cells positive for human nectin1 and HVEM, and the ovary (SK-OV-3), mammary (MCF-7) carcinoma cells and SJ-Rh4 rhabdomyosarcoma cells, expressing HER-2 at high, intermediate-low, and undetectable levels, respectively (Fig. S2). R-LM249 exhibited a highly restricted tropism for the highly HER-2–positive SK-OV-3 cells. It barely infected MCF-7 cells, and failed to infect SJ-Rh4 cells, and cells positive for nectin1 and HVEM, implying that HER-2-dependent entry requires a high level of HER-2-cell surface

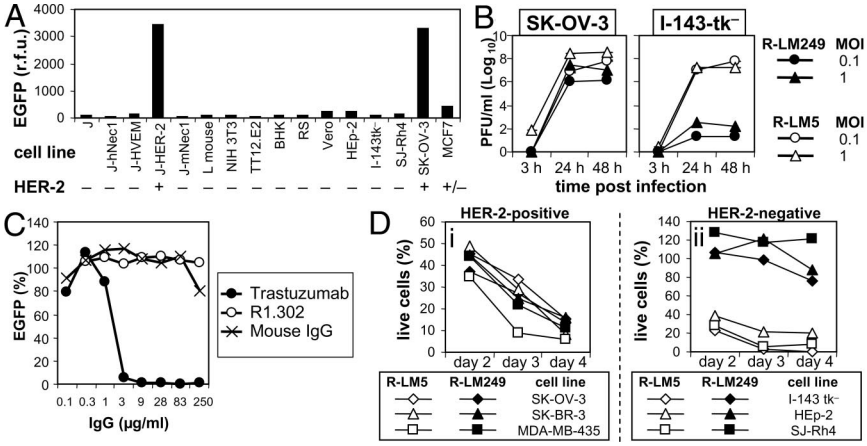

Fig. 2. R-LM249 is retargeted to HER-2 and detargeted from natural receptors. (*A*) Detection of R-LM249 infection as EGFP fluorescence 24 h after infection; fluorescence emission was measured with a fluorometer (r.f.u., relative fluorescence units). In the bottom line, − and + refer to levels of HER-2 expression. (*B*) R-LM249 and R-LM5 yield in SK-OV-3 and I-143tk$^-$ cells. Cells were infected at 0.1 or 1 pfu/cell. Progeny virus harvested at 3, 24, and 48 h after infection was titrated in SK-OV-3 cells. MOI, multiplicity of infection (pfu per cell). (*C*) Dose-dependent inhibition of R-LM249 infection into SK-OV-3 cells by trastuzumab, mAb R1.302 to nectin1, or nonimmune mouse IgGs. (*D*) Cytotoxicity of R-LM249 and R-LM5 for HER-2-positive (*i*) or HER-2-negative (*ii*) cells. Cells were infected with 3 pfu/cell. Cytotoxicity was measured at the indicated days after infection by the Erythrosin B exclusion assay.

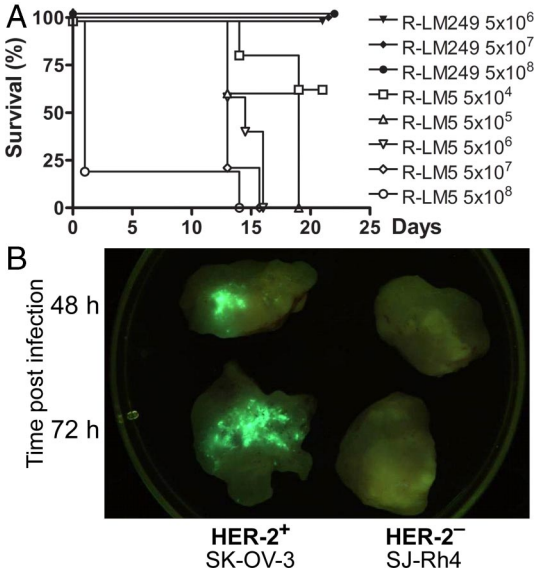

Fig. 3. R-LM249 infection in mice. (*A*) Kaplan–Meier survival curve of nude mice injected i.p. with R-LM249 or R-LM5. Five mice were injected for each dose. Two additional doses of R-LM249 (5×10^5 and 5×10^4) left all mice alive. (*B*) In vivo R-LM249 replication visualized as EGFP fluorescence. Each tumor specimen was obtained from 1 nude mouse at the indicated time after i.t. injection with R-LM249 (2×10^7 pfu per mouse). Resected tumors were cut in half to expose the inner part, placed in a 60-mm Petri dish, and observed under a fluorescent in vivo imager.

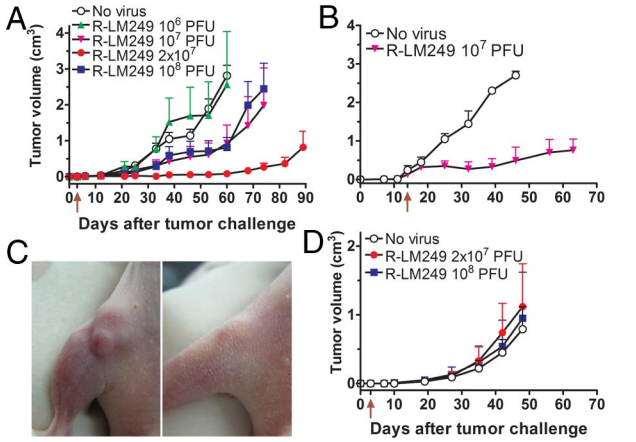

Fig. 4. Antitumor efficacy and specificity of R-LM249. Nude mice bearing progressive HER-2-positive (SK-OV-3) or HER-2-negative (SJ-Rh4) tumors were exposed i.t. to R-LM249. (*A*) Each point represents mean tumor volume ± SEM of 5 nude mice receiving R-LM249 i.t. 3 days (arrow below *x* axis) after the s.c. injection of SK-OV-3 cells. Statistical significance of difference vs. "No virus" group (Student's *t* test): 10^6, not significant; 10^7 and 10^8, $P < 0.05$ from day 53; 2×10^7, $P < 0.01$ from day 21. (*B*) Each point represents mean tumor volume ± SEM of nude mice bearing a SK-OV-3 tumor treated i.t. with R-LM249. (*C*) Mouse bearing a 0.22-cm^3 SK-OV-3 tumor (*Left*) was treated i.t. with 10^8 pfu R-LM249. (*Right*) Picture taken 15 days later. (*D*) Kinetics of SJ-Rh4 s.c. tumor appearance in groups of 5–10 nude mice treated with R-LM249 as in *A*. No significant difference vs. "No virus" group.

expression (Fig. 2*A*). To substantiate these data, we compared the yield of R-LM249 with that of R-LM5. Both viruses grew efficiently in SK-OV-3 cells, whereas R-LM249 failed to replicate above background level in I-143tk$^-$ cells (Fig. 2*B*). Last, we determined the specificity of receptor usage by dose-dependent inhibition of R-LM249 infection by trastuzumab, the humanized mAb to HER-2 used in clinical settings. In parallel, we measured the effect of mAb R1.302 to nectin1. Fig. 2*C* shows that R-LM249 infection was impaired in a dose-dependent manner by trastuzumab; mAb R1.302 exerted no effect. The results provide evidence that R-LM249 is retargeted to HER-2 and detargeted from nectin1 and HVEM.

R-LM249 Lytic Activity for Cultured Cells. To measure R-LM249 lytic activity, and to further strengthen evidence for R-LM249 specificity, we compared the lytic activity R-LM249 with that of R-LM5 for a number of cells that express HER-2 at different extents. Lysis was measured by means of the erythrosin dye exclusion test. R-LM249 was cytotoxic for all of the HER-2-positive cells, and was not cytotoxic for HER-2-negative I-143tk$^-$, HEp-2 and SJ-Rh4 cells. By contrast, R-LM5 was cytotoxic for any cell type, as expected, given that all cells carry the natural HSV receptors (Fig. 2*D*).

In Vivo Safety Profile of R-LM249. To ascertain whether full retargeting of R-LM249 was exhibited also in vivo, we compared its lethal dose 50 (LD_{50}) with that of R-LM5, after i.p. administration in amounts from 5×10^4 to 5×10^8 pfu. Mice were kept under examination for 21 days; the survivors were then killed. The Kaplan–Meier survival plot showed a pfu/LD_{50} of $\approx 5 \times 10^4$ for R-LM5, in substantial agreement with estimations for WT-HSV. None of the mice exposed to R-LM249, even those that received 5×10^8 pfu, died or showed signs of toxicity or neuroinvasiveness (Fig. 3*A*).

Intratumor Replication of R-LM249. To visualize in vivo replication and target specificity, nude mice bearing HER-2-positive or HER-2-negative human tumors were injected with R-LM249, and analyzed for R-LM249-encoded EGFP 6, 48, and 72 h after intratumoral (i.t.) inoculation. Whereas at early time (6 h) after inoculation only a few cells exhibited EGFP as expected, fluorescence was readily recorded in HER-2–positive tumors 48 and 72 h after inoculation (Fig. 3*B*). The HER-2-negative tumor did not show sign of infection at any time.

Antitumor Activity of R-LM249 in Vivo. To assess the in vivo antitumor potential of R-LM249, nude mice received SK-OV-3 cells s.c. and, 3 days later, escalating doses of R-LM249 from 10^6 to 10^8 pfu in the same site. SK-OV-3 cells were chosen, because they hyperexpress HER-2, yet are relatively resistant to trastuzumab because of defects in some intracellular signaling steps of trastuzumab response (28), a phenotype shared with trastuzumab-resistant tumors in patients (18). R-LM249 inhibited tumor growth at multiplicities $>10^6$ pfu, and led to a 20% of tumor-free mice in each group (Fig. 4*A*). The most effective dose, 2×10^7 pfu, strongly reduced growth of all tumors, which remained <0.1 cm^3 for up to 2 months after cell injection.

In a next series of experiments, a single R-LM249 treatment was delayed until tumors reached a volume of ≈ 0.2 cm^3. R-LM249 inhibited the growth of tumors that remained <1 cm^3 for >1 month after virus treatment (Fig. 4*B*). Larger tumor masses, ranging from 0.3 up to 0.6 cm^3, did not exhibit appreciable regression in size. Fig. 4*C* exemplifies a tumor of 0.2 cm^3 volume that regressed almost entirely after treatment with R-LM249. We did not detect by FACS analysis evidence of HER-2-loss tumor cell variants among untreated or R-LM249-treated SK-OV-3 tumors.

The in vivo specificity of R-LM249 was documented by failure to impair the growth of a HER-2–negative tumor, human rhabdomyosarcoma SJ-Rh4, even at 10^8 pfu (Fig. 4*D*).

To further prolong tumor inhibition, we exposed HER-2-positive tumors to repeated virus administrations. Fig. 5*A* shows that repeated administrations of an effective dose of R-LM249 resulted in a significant increase in the proportion of tumor-free mice, which reached 60% and remained stable up to 7 months

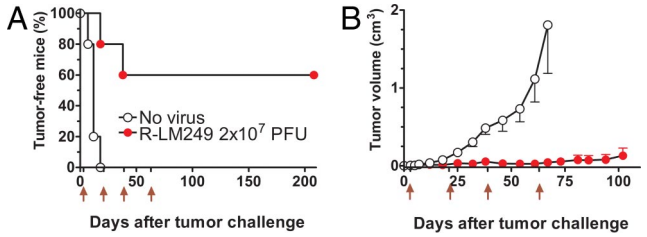

Fig. 5. Effect of repeated R-LM249 administrations on tumor growth. Groups of 5 nude mice received the s.c. injection of HER-2-positive SK-OV-3 cells and were repeatedly treated with R-LM249 at days 3, 21, 39, and 63 (red arrows below *x*-axis). (*A*) Tumor-free survival time (Kaplan–Meier analysis). Tumor-free survival of R-LM249-treated mice was significantly different from that of "No virus" group ($P < 0.005$ by the Mantel-Haenszel test). (*B*) Tumor growth curves, each point represents mean tumor volume ± SEM of 5 nude mice (including tumor-negative mice). All time points after day 18 were significantly different ($P < 0.01$ by the Student's *t* test).

of age, i.e., 5 months after the last treatment. Then, tumor-free mice were killed, and absence of tumor mass was confirmed by a very accurate necropsy and examination at low magnification under white light and at 488 nm (to detect possible EGFP expression). The tumor-bearing R-LM249-treated mice (40%) displayed only <1 cm^3 tumor masses up to at least 2 months after the last treatment (Fig. 5*B*).

Discussion

The previously undescribed findings to emerge from this study are 2-fold: (*i*) a molecular strategy to engineer a HSV fully retargeted to a receptor of choice (in this instance, HER-2) and unable to revert to WT-receptor usage; and (*ii*) the first demonstration that a retargeted HSV effectively and specifically inhibited the growth of HER-2-expressing human tumors in nude mice. Relevant to interpret the significance and potential of current work are the following considerations.

The strategy to simultaneously obtain retargeting to HER-2 and irreversible detargeting consisted in the replacement of HSV gD Ig-folded core (corresponding to half of gD ectodomain) with another Ig-folded molecule, the scFv to HER-2. Although we have no direct proof, we assume that detargeting from both receptors resulted from conformational changes consequent to the large replacement, and, for nectin1, from deletion of key residues (e.g., residue 215) (29). Importantly, the use of scFv potentially allows to target any selected cellular receptor, and current strategy can be readily applied to retarget HSV to widely differing receptor families, including EGFR, EGFRvIII, mutant HER-2, prostate specific membrane antigen (PSMA), carcinoembryonic antigen (CEA), etc. Additional key properties of R-LM249, and likely of viruses generated by this strategy, are ability to obtain virus stocks with titers of 10^9 pfu/Roller bottle, sufficiently high for preclinical evaluations, and the fact that the scFv ligand is encoded in the virus genome and displayed on virion envelope from one generation to the other.

With respect to in vivo efficacy, R-LM249 can effectively and specifically inhibit the in vivo growth of HER-2-hyperexpressing human tumor cells. A single administration exerted a distinct therapeutic effect against progressive HER-2-positive SK-OV-3 tumors up to 0.2 cm^3, which in a young nude mouse is equivalent to ≈1% of body weight. The therapeutic effect persisted for several weeks. Repeated virus administrations resulted in a high proportion of tumor-free mice for the time interval of examination (up to 5 months after the last treatment), whereas the remaining mice showed a strongly delayed tumor growth. Antitumor effect was already observed with 10^7 pfu per mouse, a dose effectively used with other oncolytic HSV in mice (30, 31), and comparable, after body surface area normalization, with 3×10^9 pfu used in some clinical trials (32). Surprisingly, 10^8 pfu was less effective than 2×10^7 pfu, possibly because concentrated virions aggregated in the mice tissue, thus, reducing the effective dose, or because they caused an immediate apoptosis of target cells, thus, reducing the reservoir of cells where the virus can replicate and spread to other cells (33).

The safety profile of R-LM249 is documented by the very high LD_{50} ($>5 \times 10^8$ pfu) as compared with $\approx 5 \times 10^4$ for R-LM5 carrying WT-gD; its replication and spread limited to the HER-2-hyperexpressing cells; the fact that the virus self-exhausts once it has infected and lysed the tumor cells and encounters the adjacent nontumor tissue, and cannot revert to WT-tropism. Indeed, in the worst-case scenario, double infection and recombination between WT-HSV and the retargeted virus may, at maximum, generate the 2 viruses themselves. However, R-LM249 inability to infect cells that express HER-2 at low-intermediate level ensures that any nontumor cell constitutively expressing this molecule is spared by the virus. Such high safety profile cannot be obtained with recombinants that carry 2 copies of the glycoprotein, 1 WT and 1 retargeted (34).

R-LM249 efficacy in immunocompetent animals remains to be determined. In principle, although the immune system facilitates tumor clearance, prior immunity to virus might decrease its efficacy. Preclinical and clinical studies argue that prior immunity to HSV does not represent an obstacle. Thus, intravenously administered $\gamma_1$34.5-deleted HSV was effective in prostate and pulmonary tumor models, irrespective of whether mice were previously immunized with HSV (35, 36). In phase I clinical trials, $\gamma_1$34.5-deleted HSV was administered i.t. in various tumors, and stereotactically in gliomas; a therapeutic effect was noticed irrespective of the serostatus or seroconversion of patients (2, 3).

As compared with other candidate oncolytic viruses (4, 5, 8), HSV offers some advantages. Its ample genome can accommodate additional therapeutic and immunomodulatory genes to arm the oncolytic virus (3, 37). The tumor-selective G207, deleted in $\gamma_1$34.5 gene, proved to be very safe when injected intracerebrally in humans in amounts as high as 10^9 pfu, testifying the lack of HSV toxicity even when injected in its target organ. A retargeted HSV could be easily converted into a virus suitable for imaging and metastases detection (38). HSV persists in most of the human population worldwide, and generally causes no-to-mild pathologies; any unwanted virus replication can be blocked by acyclovir.

The clinical relevance of HER-2-hyperexpressing carcinomas is underscored by their world-wide incidence, and the fact that only a subset responds to current therapy. Also, the majority of patients who initially respond to trastuzumab become resistant within 1 year of treatment initiation (18). Although there is a pressing need for novel therapeutic approaches, so far, few efforts were undertaken to generate HER-2-specific oncolytic viruses or lytic immune cells (19, 39). Such viruses share their target with small molecule inhibitors (SMI) and, particularly, mAbs. However, retargeted viruses offer distinct advantages over traditional therapeutic endeavors. Self-replication of the therapeutic agent is a unique property that enables therapeutic viruses to compete with proliferating cancer cells without the half-life limitations of SMI and mAbs. Also, data here reported with a relatively HER-2 resistant target tumor suggest that therapy with oncolytic viruses retargeted by means of scFv fragments can be an effective tool for treatment of patients with resistant tumor cells. Proposed mechanisms of tumor resistance to trastuzumab affect HER-2 signaling rather than its surface expression (18); thus, leaving an intact target for HER-2-redirected oncolytic viruses. Clinical evidence indicates that trastuzumab controls metastatic growth in many sites, but not in the brain, because antibodies do not cross the blood–brain barrier (40). Therefore, a foreseeable application could be the therapy of brain metastases inaccessible to trastuzumab; in such

localized administration, HSV would find an ideal application, and would be shielded from systemic immunity. Retargeted HSVs could provide effective therapeutic advances over the unretargeted HSVs, possibly in combinatorial or sequential protocols with SMI and mAbs against the same or complementary therapeutic targets.

Methods

Cells and Viruses. SK-OV-3 (ovarian carcinoma), SK-BR-3, and MDA-MB-453 (mammary carcinoma) exhibit very high HER-2 expression. MCF-7 (mammary carcinoma) and SJ-Rh4 (rhabdomyosarcoma) exhibit low/intermediate or null HER-2 expression, respectively (41). TT12.E2 (derived from a mammary carcinoma of rat HER-2/neu transgenic mice), exhibiting very high expression of rat HER-2/neu, was used as specificity control. Further cells lines were J, J-hNectin1 (human), J-mNectin1 (murine), J-HVEM, J-HER-2 (26), L, NIH 3T3, BHK, RS, Vero, I-143tk$^-$, and HEp-2. Cells were cultured in DMEM supplemented with 5–10% FBS (Invitrogen). R-LM249 and R-LM5 viruses were grown in SK-OV-3 or BHK cells, respectively, and titrated in SK-OV-3 cells by plaque assay. Experiments in mice were carried out with extracellular viruses harvested by high-speed centrifugation through a sucrose cushion.

Infection Assays. Cells in 96-well plates were infected at 5 pfu/cell in duplicate. Infection was monitored 24 h later as EGFP expression, by Synergy HTTR-I fluorometer (Bio-TEK).

Inhibition of Virus Infection. SK-OV-3 cells in 96-well plates were exposed to increasing concentrations of purified antibodies (R1.302 to nectin1, trastuzumab to HER-2, or mouse immunoglobulins), and then to R-LM249 (2 pfu/cell) in the presence of Abs, as detailed (26).

Virus Replication Assay. SK-OV-3 and I-143tk$^-$ cells in 12-well plates were infected at 0.1 or 1 pfu/cell, and frozen at 3, 24, or 48 h after infection. Progeny virus (intracellular plus extracellular) was titrated in SK-OV-3 cells, as detailed (26).

In Vitro Cytotoxicity. Cells were seeded in 12-well plates, infected the day after at 3 pfu/cell, or left uninfected. At different time points cells were trypsinized and collected, and the number of viable and nonviable cells was determined by means of the Erythrosin B (Sigma–Aldrich) dye exclusion assay. The number of viable cells (Erythrosin negative) in infected samples was expressed as percentage of viable cells versus the respective uninfected sample.

Tumor Growth. Athymic Crl:CD1-*Foxn1^{nu}* (referred to as nude) mice were purchased from Charles River, and maintained under sterile conditions. Experiments were authorized by the institutional review board of the University of Bologna, and were performed according to Italian and European guidelines. Groups of individually tagged virgin female nude mice of 6 weeks of age received the s.c. injection of a tumorigenic dose of SK-OV-3 cells (2×10^6 cells) or SJ-Rh4 cells (30×10^6 cells) in 0.2 mL PBS. Tumor growth was assessed weekly by measuring with a caliper, tumor volume was calculated as $\pi[\sqrt{(a \cdot b)}]^3/6$, where a = maximal tumor diameter, and b = tumor diameter perpendicular to a. To perform cytofluorometric analysis, tumor samples, washed in PBS, were mechanically and enzymatically dissociated (0.5 mg/mL trypsin, 0.2 mg/mL EDTA; Invitrogen) at 37 °C for 5 min. Cell suspension was filtered across a 70-μm cell strainer (Falcon Plastics).

In Vivo Infection. Mice with SK-OV-3 or SJ-RH4 s.c. tumors received an i.t. injection of R-LM249 in 0.2 mL PBS, and were killed 6, 48, and 72 h later. Resected tumors were cut in half and observed under a fluorescent in vivo imager (Lightools Research). Accurate observation of other organs did not reveal any fluorescence.

Antitumor Activity. At 3 days after tumor cell injection or at definite tumor volumes, mice were randomized in groups of 5–10, and R-LM249 injected in 0.2 mL PBS in tumor site or i.t. ''No virus'' control groups, run in parallel, consisted of mice untreated and treated with PBS only (not statistically different). Latency time corresponded to a tumor mass $\geq$0.03 cm^3. Tumor volumes for each group and time were calculated as mean $\pm$ SE, until all mice of the group were alive.

Statistical Analysis. Tumor-free survival curves (Kaplan–Meier) were compared by the Mantel-Haenszel test. Tumor volumes were compared by the Student's *t* test.

Additional Details. For more details, see *SI Materials and Methods*.

ACKNOWLEDGMENTS. We thank Genentech for gift of trastuzumab and cDNA encoding HER-2 scFv, and Elisabetta Romagnoli for assistance with cell and virus cultures. The work was supported by the TargetHerpes European Union Grant LSHG-CT-2006-037517 (to G.C.-F.), Progetti di Ricerca di Interesse Nazionale-Ministero dell'Istruzione, dell'Università e della Ricerca, the University of Bologna (Ricerca Fondamentale Orientata), grants from Fondo Pallotti and Alma Medicina, and the Federation of European Microbiological Societies-European Society of Clinical Microbiology and Infectious Diseases Fellowship 2006-1 (to L.M.).

1. Martuza RL, Malick A, Markert JM, Ruffner KL, Coen DM (1991) Experimental therapy of human glioma by means of a genetically engineered virus mutant. *Science* 252:854–856.
2. Markert JM, Gillespie GY, Weichselbaum RR, Roizman B, Whitley RJ (2000) Genetically engineered HSV in the treatment of glioma: A review. *Rev Med Virol* 10:17–30.
3. Hu JC et al. (2006) A phase I study of OncoVEXGM-CSF, a second-generation oncolytic herpes simplex virus expressing granulocyte macrophage colony-stimulating factor. *Clin Cancer Res* 12:6737–6747.
4. Cattaneo R, Miest T, Shashkova EV, Barry MA (2008) Reprogrammed viruses as cancer therapeutics: Targeted, armed and shielded. *Nat Rev Microbiol* 6:529–540.
5. Guo ZS, Thorne SH, Bartlett DL (2008) Oncolytic virotherapy: Molecular targets in tumor-selective replication and carrier cell-mediated delivery of oncolytic viruses. *Biochim Biophys Acta* 1785:217–231.
6. Blechacz B, Russell SJ (2008) Measles virus as an oncolytic vector platform. *Curr Gene Ther* 8:162–175.
7. Li QX, Liu G, Wong-Staal F (2008) Oncolytic virotherapy as a personalized cancer vaccine. *Int J Cancer* 123:493–499.
8. Brower V (2008) Cancer-killing viruses assist gene therapies. *J Natl Cancer Inst* 100:1350–1351.
9. Prestwich RJ, Harrington KJ, Vile RG, Melcher AA (2008) Immunotherapeutic potential of oncolytic virotherapy. *Lancet Oncol* 9:610–612.
10. Zhou G, Ye GJ, Debinski W, Roizman B (2002) Engineered herpes simplex virus 1 depends on IL13Ralpha2 receptor for cell entry and independent of glycoprotein D receptor interaction. *Proc Natl Acad Sci USA* 99:15124–15129.
11. Nakamura T, et al. (2005) Rescue and propagation of fully retargeted oncolytic measles viruses. *Nat Biotechnol* 23:209–214.
12. Zhou G, Roizman B (2006) Construction and properties of a herpes simplex virus 1 designed to enter cells solely via the IL-13alpha2 receptor. *Proc Natl Acad Sci USA* 103:5508–5513.
13. Gao Y, Whitaker-Dowling P, Griffin JA, Barmada MA, Bergman I (2008) Recombinant vesicular stomatitis virus targeted to Her2/neu combined with anti-CTLA4 antibody eliminates implanted mammary tumors. *Cancer Gene Ther* 16:44–52.
14. Gonzalez-Angulo AM, Hortobagyi GN, Esteva FJ (2006) Adjuvant therapy with trastuzumab for HER-2/neu-positive breast cancer. *Oncologist* 11:857–867.
15. Ross JS, et al. (2003) The Her-2/neu gene and protein in breast cancer 2003: Biomarker and target of therapy. *Oncologist* 8:307–325.
16. Hynes NE, Lane HA (2005) ERBB receptors and cancer: The complexity of targeted inhibitors. *Nat Rev Cancer* 5:341–354.
17. Baselga J, Perez EA, Pienkowski T, Bell R (2006) Adjuvant trastuzumab: A milestone in the treatment of HER-2-positive early breast cancer. *Oncologist* 1:4–12.
18. Nahta R, Yu D, Hung MC, Hortobagyi GN, Esteva FJ (2006) Mechanisms of disease: Understanding resistance to HER2-targeted therapy in human breast cancer. *Nat Clin Pract Oncol* 3:269–280.
19. Bergman I, Griffin JA, Gao Y, Whitaker-Dowling P (2007) Treatment of implanted mammary tumors with recombinant vesicular stomatitis virus targeted to Her2/neu. *Int J Cancer* 121:425–430.
20. Belousova N, Mikheeva G, Gelovani J, Krasnykh V (2008) Modification of adenovirus capsid with a designed protein ligand yields a gene vector targeted to a major molecular marker of cancer. *J Virol* 82:630–637.
21. Cocchi F, Menotti L, Mirandola P, Lopez M, Campadelli-Fiume G (1998) The ectodomain of a novel member of the immunoglobulin superfamily related to the poliovirus receptor has the attibutes of a *bonafide* receptor for herpes simplex viruses 1 and 2 in human cells. *J Virol* 72:9992–10002.
22. Geraghty RJ, Krummenacher C, Cohen GH, Eisenberg RJ, Spear PG (1998) Entry of alphaherpesviruses mediated by poliovirus receptor-related protein 1 and poliovirus receptor. *Science* 280:1618–1620.
23. Campadelli-Fiume G, et al. (2007) The multipartite system that mediates entry of herpes simplex virus into the cell. *Rev Med Virol* 17:313–326.
24. Spear PG, et al. (2006) Different receptors binding to distinct interfaces on herpes simplex virus gD can trigger events leading to cell fusion and viral entry. *Virology* 344:17–24.
25. Menotti L, Cerretani A, Campadelli-Fiume G (2006) A herpes simplex virus recombinant that exhibits a single-chain antibody to HER2/neu enters cells through the mammary tumor receptor, independently of the gD receptors. *J Virol* 80:5531–5539.
26. Menotti L, Cerretani A, Hengel H, Campadelli-Fiume G (2008) Construction of a fully retargeted herpes simplex virus 1 recombinant capable of entering cells solely via human epidermal growth factor receptor 2. *J Virol* 20:10153–10161.
27. Zhou G, Roizman B (2007) Separation of receptor binding and pro-fusogenic domains of glycoprotein D of herpes simplex virus 1 into distinct interacting proteins. *Proc Natl Acad Sci USA* 104:4142–4146.

28. Longva KE, Pedersen NM, Haslekas C, Stang E, Madshus IH (2005) Herceptin-induced inhibition of ErbB2 signaling involves reduced phosphorylation of Akt but not endocytic down-regulation of ErbB2. *Int J Cancer* 116:359–367.
29. Manoj S, Jogger CR, Myscofski D, Yoon M, Spear PG (2004) Mutations in herpes simplex virus glycoprotein D that prevent cell entry via nectins and alter cell tropism. *Proc Natl Acad Sci USA* 101:12414–12421.
30. Kooby DA, et al. (1999) Oncolytic viral therapy for human colorectal cancer and liver metastases using a multi-mutated herpes simplex virus type-1 (G207). *FASEB J* 13:1325–1334.
31. Liu R, Varghese S, Rabkin SD (2005) Oncolytic herpes simplex virus vector therapy of breast cancer in C3(1)/SV40 T-antigen transgenic mice. *Cancer Res* 65:1532–1540.
32. Markert JM, et al. (2000) Conditionally replicating herpes simplex virus mutant, G207 for the treatment of malignant glioma: Results of a phase I trial. *Gene Ther* 7:867–874.
33. Leopardi R, Roizman B (1996) The herpes simplex virus major regulatory protein ICP4 blocks apoptosis induced by the virus or by hyperthermia. *Proc Natl Acad Sci USA* 93:9583–9587.
34. Conner J, Braidwood L, Brown SM (2008) A strategy for systemic delivery of the oncolytic herpes virus HSV1716: Redirected tropism by antibody-binding sites incorporated on the virion surface as a glycoprotein D fusion protein. *Gene Ther* 15:1579–1592.
35. Wong RJ, et al. (2004) Effective intravenous therapy of murine pulmonary metastases with an oncolytic herpes virus expressing interleukin 12. *Clin Cancer Res* 10:251–259.
36. Varghese S, et al. (2007) Systemic therapy of spontaneous prostate cancer in transgenic mice with oncolytic herpes simplex viruses. *Cancer Res* 67:9371–9379.
37. Parker JN, et al. (2000) Engineered herpes simplex virus expressing IL-12 in the treatment of experimental murine brain tumors. *Proc Natl Acad Sci USA* 97:2208–2213.
38. Burton JB, et al. (2008) Adenovirus-mediated gene expression imaging to directly detect sentinel lymph node metastasis of prostate cancer. *Nat Med* 14:882–888.
39. Kruschinski A, et al. (2008) Engineering antigen-specific primary human NK cells against HER-2 positive carcinomas. *Proc Natl Acad Sci USA* 105:17481–17486.
40. Melisko ME, Glantz M, Rugo HS (2009) New challenges and opportunities in the management of brain metastases in patients with ErbB2-positive metastatic breast cancer. *Nat Clin Pract Oncol* 6:25–33.
41. Ricci C, et al. (2002) HER/erbB receptors as therapeutic targets of immunotoxins in human rhabdomyosarcoma cells. *J Immunother* 25:314–323.
42. Krummenacher C, et al. (2005) Structure of unliganded HSV gD reveals a mechanism for receptor-mediated activation of virus entry. *EMBO J* 24:4144–4153.
43. Humphrey W, Dalke A, Schulten K (1996) VMD: Visual molecular dynamics. *J Mol Graphics* 14:33–38:27–38.